

Characterisation of Nd-doped calcium aluminosilicate parent glasses designed for the preparation of zirconolite-based glass-ceramic waste forms

P. Loiseau¹, D. Caurant¹, K. Dardenne², S. Mangold³, M. Denecke², J. Rothe², N. Baffier¹, C. Fillet⁴

¹ LCAES (CNRS UMR 7574), ENSCP, 11 rue P. et M. Curie, 75231 Paris Cedex 05, France
pascal-loiseau@enscp.jussieu.fr

² Forschungszentrum Karlsruhe GmbH, INE, Hermann-von-Helmoltz-Platz, D-76344 Eggenstein-Leopoldshafen, Germany

³ Forschungszentrum Karlsruhe GmbH, ISS, Hermann-von-Helmoltz-Platz, D-76344 Eggenstein-Leopoldshafen, Germany

⁴ CEA/DEN/DIEC/SCDV, 30207 Bagnols-sur-Cèze, France

Abstract – Zirconolite-based (nominally $\text{CaZrTi}_2\text{O}_7$) glass-ceramics belonging to the $\text{SiO}_2\text{-Al}_2\text{O}_3\text{-CaO-ZrO}_2\text{-TiO}_2$ system are good waste forms for the specific immobilisation of actinides. The understanding of their crystallisation processes implies to investigate the structure of the glass. Thus, the environment around Ti, Zr (nucleating agents) and Nd (trivalent actinides surrogate) was characterised in parent glasses. Electron spin resonance (ESR) study of the small amount of Ti^{3+} occurring in the glass enabled to identify two types of sites for titanium: the main one is of C_{4v} or D_{4h} symmetry. EXAFS showed that Zr occupied a quite well defined 6-7-fold coordinated site with second neighbours which could correspond to Ca/Ti and Zr. Nd environment was probed by optical spectroscopies (absorption, fluorescence), ESR and EXAFS. All these techniques demonstrated that the environment around Nd was very constrained by the glassy network. Notably, Nd occupies a highly distorted 8-9-fold coordinated site in the parent glass.

INTRODUCTION

Zirconolite ($\text{CaZrTi}_2\text{O}_7$) is a naturally occurring phase which exhibits an excellent chemical durability and a good actinide containment capacity. Therefore, this crystalline phase is a waste form of choice for the specific immobilisation of minor actinides (mainly responsible for the long-term radiotoxicity of reprocessed high level nuclear waste) or of plutonium. An alternative to the ceramic route is to prepare zirconolite crystals by controlled crystallisation (nucleation+growth) of a parent glass. This glass-ceramic route is simpler to implement in radioactive plants and offers a greater chemical flexibility against waste composition fluctuations due to the presence of a residual glass surrounding zirconolite crystals.

The basic parent glass composition which was studied is as follows (mol. %): 48.8 SiO_2 , 8.5 Al_2O_3 , 25.3 CaO , 11.3 TiO_2 , 5.0 ZrO_2 , 1.1 Na_2O . This composition was determined from [1] and various loadings of Nd_2O_3 (trivalent actinide surrogate) were added up to 2.2 mol. % (10 wt. %). Previous studies showed that such glasses led to the only crystallisation of zirconolite in their bulk by controlled crystallisation (nucleation + crystal growth) [2]. However, the understanding of crystallisation processes implies to investigate the structure of the glass if further composition optimisations are to perform. This is why the environment around three

elements was characterised in these parent glasses: Ti and Zr (which play a key role in nucleation processes and which are main components of zirconolite), and Nd.

EXPERIMENTAL

40g batch glasses were prepared following a standard method comprising two stages of melting and casting at 1550°C with intermediate grinding in order to increase glass homogeneity. Their compositions were checked by ICP-AES and they were perfectly amorphous. A similar glass transformation temperature around 760 °C was found for all the glasses (measured by differential thermal analysis), which means that the addition of Nd_2O_3 up to 2.2 mol. % has no significant effect on the mean bond strength of the glassy network.

Due to the high preparation temperature of the glasses, a small quantity of Ti^{4+} ions are reduced into Ti^{3+} state. Contrarily to Ti^{4+} ions, Ti^{3+} ions ($3d^1$ electron configuration) can be detected by Electron Spin Resonance (ESR). Ti^{3+} ESR measurements were performed at 120 K using a Bruker ESP 300e spectrometer operating at X-band ($\nu \approx 9.5$ GHz).

Room temperature EXAFS (Extended X-ray Absorption Fine Structure) measurements were performed at Zr-K edge (17998 eV) and Nd- L_3 edge (6208 eV) at ANKA synchrotron

(Germany, Karlsruhe) in transmission mode through quenched glass samples containing 1.3 mol. % of Nd_2O_3 (6 wt. %) dispersed in boron nitride pellets. EXAFS signals were extracted and simulated using the UWXAFS package [3]. Nd^{3+} optical properties were characterised at 15 K by absorption from 400 to 900 nm and by emission from 860 to 960 nm ($^4\text{F}_{3/2} \rightarrow ^4\text{I}_{9/2}$ channel). At 15 K, only the lowest energy Kramers doublet of the $^4\text{I}_{9/2}$ or of the $^4\text{F}_{3/2}$ multiplet is populated for absorption or emission measurements respectively.

RESULTS AND DISCUSSION

ESR study of native Ti^{3+} ions in parent glass

During glass melting, a $\text{Ti}^{4+} \rightleftharpoons \text{Ti}^{3+}$ equilibrium was established (displaced towards reduction with increasing temperature) and then was frozen by quenching at room temperature. Therefore, a small quantity of Ti^{3+} , detected by ESR (Fig. 1), formed. Their amount was quantified by ESR at 120 K with a DPPH standard. For all the glasses, it was shown that the proportion of Ti at the trivalent oxidation state was below 0.7 ppm (case of the undoped glass) and decreased with increasing Nd_2O_3 concentration (no Ti^{3+} ion detected for the 10 wt. % Nd_2O_3 glass). Such an evolution is difficult to explain (Nd only exists as Nd^{3+} ion) but could result from an increase of the glass basicity [4] with Nd concentration, if we admit that Nd acts as a network modifier.

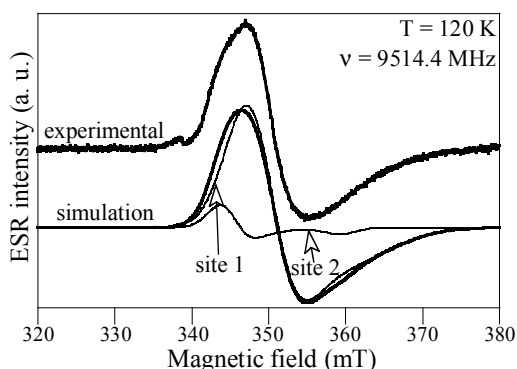


Fig. 1. Experimental and simulated Ti^{3+} ESR signal for the undoped glass.

Ti^{3+} ESR signal was simulated with the assumption of an axial symmetry for simplicity reasons. Without taking into account any distribution of g factor, it was necessary to consider two contribution (with gaussian line shape) to simulate the signal and the shoulder

occurring around 344 mT. This gives evidence of two types of sites for Ti^{3+} ions in the glass, referred as site 1 and site 2. Results of the simulation for the undoped glass are shown in Fig. 1 and Table I. Site 2 contributes only to 8.5 % of the overall signal.

TABLE I. Results of the ESR simulation.

	g_{\perp}	FWHM	g_{\parallel}	FWHM
Site 1	1.946	6.5 mT	1.88	12 mT
Site 2	1.973	4 mT	1.89	4 mT

The knowledge of the g factors gives pieces of information about the symmetry of Ti^{3+} environment in the glass [5]. As Ti^{3+} ESR signal can be detected at room temperature, several simple geometries can be excluded: tetrahedron, octahedron and tetragonally elongated octahedron. A compressed tetrahedral symmetry can also be excluded because it would imply $g_{\perp} < g_{\parallel}$. An elongated tetrahedral symmetry would impose $(g_{\parallel} - g_c)/(g_{\perp} - g_c) = 4$ ($g_c = 2.0023$), which could only be verified by the site 2, although a four-fold coordination is quite unlikely for a cation as big as Ti^{3+} ($r_{\text{VI}}(\text{Ti}^{3+}) = 0.67 \text{ \AA} > r_{\text{VI}}(\text{Ti}^{4+}) = 0.605 \text{ \AA}$ [6]).

However, ESR results can be fully explained by considering a compressed octahedral symmetry, highly distorted to have the order $g_{\parallel} < g_{\perp}$ (more distorted for site 2). This geometry could correspond either to a C_{4v} or a D_{4h} symmetry (5 to 6 coordination number). It is interesting to notice that the C_{4v} symmetry is the one of the square pyramidal $\text{O}=\text{TiO}_4$ frequently proposed for Ti^{4+} environment in glasses [7].

EXAFS characterisation of Zr^{4+} environment in parent glass

The short range order around Zr in the 6 wt. % Nd_2O_3 parent glass was determined from the simulation of the EXAFS spectrum recorded at room temperature (Fig. 2). Zr occupies a well defined site (debye-waller factor $\sigma^2 = 0.007 \pm 0.001 \text{ \AA}^{-2}$ of 6.5 ± 0.7 coordination number with a consistent mean Zr-O distance $d(\text{Zr-O}) = 2.15 \pm 0.02 \text{ \AA}$. This result shows that Zr^{4+} ion is able to impose its own environment in the glass. This environment is relatively close to the one which was reported in literature for a depolymerised glass such as R7T7 glass, with a coordination number around 6 and a mean Zr-O distance ranging from 2.07 to 2.10 \AA [8]. The fact that slightly higher coordination number and Zr-O distance were found in our glass could be due to

the higher polymerisation of the glassy network. For 100 moles of undoped glass, assuming that Al, Ti and Zr adopt respectively the geometries $(\text{AlO}_4)^-$, $(\text{O}=\text{TiO}_4)^{2-}$ and $(\text{ZrO}_6)^{2-}$, 24.7 moles of $(\text{CaO} + \text{Na}_2\text{O})$ would be mobilised for their charge compensation, so that only 1.7 moles of $(\text{CaO} + \text{Na}_2\text{O})$ would indeed be free to depolymerise the glassy network. In such a case, oxygens are less polarisable and a higher coordination number is required for Zr^{4+} charge shielding. In zirconolite, Zr coordination number is 7 and $d(\text{Zr}-\text{O}) = 2.20(1) \text{ \AA}$. This short range order similarity with the parent glass could predispose to zirconolite nucleation.

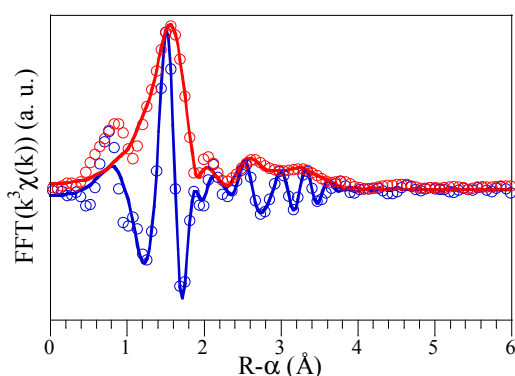


Fig. 2. Fit (solid lines) to the EXAFS (open circles) of the 6 wt. % Nd_2O_3 parent glass (Zr-K edge, room temperature).

The EXAFS analysis of the next nearest neighbours around Zr is complicated (Fig. 2): at least two shells (likely three) with overlapping shapes are necessary to simulate the spectrum, and they partly interfere destructively. Nevertheless, the Fourier peak around 3.2 \AA seems to be associated to Ca/Ti on the one hand and Zr on the other hand, both occurring at distances around 3.5 \AA from Zr.

Spectroscopic investigation of Nd^{3+} environment in parent glass

The fluorescence spectra corresponding to the $^4\text{F}_{3/2} \rightarrow ^4\text{I}_{9/2}$ Nd transition were recorded at 15 K by exciting the Nd-doped glasses at the maximum of the $^4\text{I}_{9/2} \rightarrow ^4\text{F}_{5/2} - ^2\text{H}_{9/2}$ Nd absorption band around 806.5 nm. Although the five expected emission lines cannot be resolved due to the inhomogeneous line broadening, these spectra allow to estimate the total splitting of the $^4\text{I}_{9/2}$ ground multiplet which is about 500 cm^{-1} . To compare, it was evaluated at 775 cm^{-1} for Nd-doped zirconolite samples prepared by solid state

reaction at 1460°C . The $^4\text{I}_{9/2}$ splitting is a measure of the mean crystal field experienced by Nd^{3+} ion in a host. The limit between compounds with low and high crystal field strength was set at 470 cm^{-1} by Auzel [9]. The greater crystal field of Nd in zirconolite as compared to parent glass indicates not only that the environments are different between the two hosts, but also that the mean Nd-O distance is shorter in zirconolite.

Nd optical absorption spectra were recorded for the Nd-doped glasses at 15 K. They are all very similar, even though a slight broadening of absorption lines occurs with increasing Nd_2O_3 concentration from 0.5 to 10 wt. % (Fig. 3). Three absorption bands from $^4\text{I}_{9/2}$ state are particularly interesting: towards $^2\text{P}_{1/2}$ ($\sim 23200 \text{ cm}^{-1}$), $^4\text{F}_{3/2}$ ($\sim 11400 \text{ cm}^{-1}$) and $^2\text{G}_{7/2} - ^4\text{G}_{5/2}$ ($\sim 17200 \text{ cm}^{-1}$). The first two bands ($^2\text{P}_{1/2}$ and $^4\text{F}_{3/2}$) notably give information about the variety of Nd environment because of the low degeneracy of the excited state, whereas the latter band ($^2\text{G}_{7/2} - ^4\text{G}_{5/2}$) is described as hypersensitive and is very sensitive to Nd environment. For instance, the FWHM of the $^4\text{I}_{9/2} \rightarrow ^2\text{P}_{1/2}$ band is approximately 150 cm^{-1} in Nd-doped parent glasses, much more than the one measured for zirconolite (30 cm^{-1}), which reflects a higher distribution of environment in the glasses.

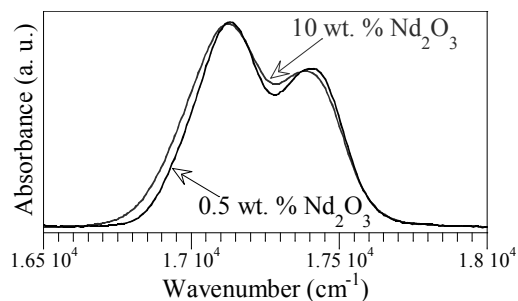


Fig. 3. Portion of Nd optical absorption spectra measured at 15 K in two parent glasses ($^4\text{I}_{9/2} \rightarrow ^2\text{G}_{7/2} - ^4\text{G}_{5/2}$ transition).

Moreover, by comparison with literature [10], the shape of the $^4\text{I}_{9/2} \rightarrow ^2\text{G}_{7/2} - ^4\text{G}_{5/2}$ is structure less (Fig. 3) and is characteristic either of highly polymerised glassy network or of glasses containing high field strength network modifiers. All these observations agree with an irregular Nd environment partly imposed by the glassy network topology, contrarily to Zr (see above).

The environment of Nd was probed by EXAFS at L_3 edge (6208 eV). The short range order around Nd in the 6 wt. % Nd_2O_3 glass was determined from the simulation of the EXAFS spectrum recorded at room temperature (Fig. 4).

Nd occupies a highly distorted site, the EXAFS simulation implies a cumulant analysis of the data (non-gaussian asymmetric Nd-O pair distribution [11]) with a large debye-waller factor $\sigma^2 = 0.029 \pm 0.001 \text{ \AA}^{-2}$. Nd-O coordination number is 8.6 ± 0.8 and the mean Nd-O distance is about $2.53 \pm 0.02 \text{ \AA}$ in the glass.

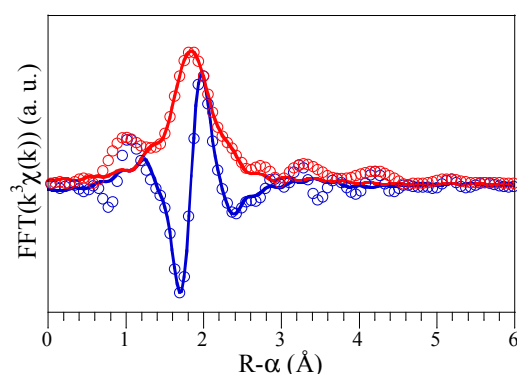


Fig. 4. Fit (solid lines) to the EXAFS (open circles) of the 6 wt. % Nd_2O_3 parent glass (Nd- L_3 edge, room temperature).

In zirconolite, Nd coordination by O is 8 and, by EXAFS, Nd-O bond distance was found to be $2.44 \pm 0.01 \text{ \AA}$ with a debye-waller factor $\sigma^2 = 0.010 \pm 0.001 \text{ \AA}^{-2}$. So, the environment around neodymium in the glass shows striking differences with the one in the zirconolite crystalline phase and is much more distorted. Therefore, the incorporation of neodymium into zirconolite crystals during devitrification will imply strong reconstructive phenomena which are assumed to occur at high temperature, when the viscosity of the supercooled liquid is significantly lowered. In these conditions, it can be inferred that neodymium did not participate actively to the earliest steps of zirconolite nucleation processes. On the contrary, neodymium increases diffusional problems and can hinder zirconolite nucleation in the parent glass.

CONCLUSION

The environment around three cations, Ti^{3+} , Zr^{4+} and Nd^{3+} was characterised by spectroscopic techniques in aluminosilicate glasses designed for the preparation of zirconolite-based glass-ceramic waste forms.

ESR study of Ti^{3+} ions formed during glass melting at 1550°C revealed that their environment could be described by a C_{4v} or D_{4h} symmetry. This could correspond to a square

pyramidal $\text{O}=\text{TiO}_4$ or to a six-fold coordinated octahedron axially compressed. The coordination numbers involved in such geometries are close to the ones encountered in zirconolite (6 and 5) which is aimed to crystallise by heat treatment of the glasses.

Zr-K edge EXAFS spectra showed that Zr^{4+} ions occupied well defined 6-7 coordinated sites, close to the ones of zirconolite. This result confirms the nucleating effect of Zr which was observed on zirconolite crystallisation in the glass.

Contrarily to Zr^{4+} ion which can be described as a cross-linking agent that reinforces the glassy network, Nd^{3+} ion must rather be considered as a network modifier or a charge compensator which exhibits a lower ability to impose its own environment in a relatively polymerised glassy network. All the optical spectroscopies and EXAFS agree to describe Nd environment as being constrained by the glassy network with coordination number and Nd-O distance significantly greater than the ones of zirconolite. Therefore, Nd^{3+} ion cannot act as a nucleating agent for zirconolite crystallisation.

REFERENCES

1. C. FILLET, J. MARILLET, J. L. DUSSOSSOY, F. PACAUD, N. JACQUET-FRANCILLION, J. PHALIPPOU, *Ceramic Transactions*, **87**, 531 (1998).
2. P. LOISEAU, D. CAURANT, O. MAJERUS, N. BAFFIER, C. FILLET, *J. Mater. Science*, **38**, 843 (2003).
3. M. NEWVILLE, *J. Synchrotron Rad.*, **8**, 96 (2001).
4. P. CLAES, *Verre*, **6**(1), 33 (2000).
5. J.E. WERTZ, J.R. BOLTON, in *Electron Spin Resonance: Elementary theory and practical applications*, Ed. McGraw-Hill, Series in Advanced Chemistry (1972).
6. R.D. SHANNON, *Acta Crystallogr.*, **A32**, 751 (1976).
7. G.E. BROWN Jr., F. FARGES, G. CALAS, *Rev. Mineral.*, **32**, 317 (1995).
8. L. GALOISY, E. PELEGRIN, M.-A. ARRIO, P. ILDEFONSE, G. CALAS, D. GHALEB, C; FILLET, F. PACAUD, *J. Am. Ceram. Soc.*, **82**(8), 2219 (1999)
9. F. AUZEL, *Mat. Res. Bull.*, **14**, 223 (1979)
10. A.A. DYMNIKOV, A.K. PRZHEVUSKII, *J. Non-Cryst. Solids*, **215**, 83 (1997)
11. G. DALBA, P. FORNASINI, F. ROCCA, *Phys. Rev. B*, **47**(14), 8502 (1993)